PAN POLSKA AKADEMIA NAUK

METROLOGY AND MEASUREMENT SYSTEMS

Index 330930, ISSN 0860-8229
www.metrology.pg.gda.pl

M&MS

IMPROVED CLASSIFICATION ROBUST KALMAN FILTERING METHOD FOR PRECISE POINT POSITIONING

Qieqie Zhang[1,2], Long Zhao[1,2], Jianhua Zhou[1,3]

1) *Beihang University, School of Automation Science and Electrical Engineering, Beijing, China* (*zhangqieqie@buaa.edu.cn*)
2) *Beihang University, Digital Navigation Center, Beijing, China* (✉ *buaa_dnc@buaa.edu.cn*, +86 010 8231 6764)
3) *Beijing Satellites Navigation Center, Beijing, China* (*julianma@263.net.cn*)

Abstract

The accuracy and reliability of Kalman filter are easily affected by the gross errors in observations. Although robust Kalman filter based on equivalent weight function models can reduce the impact of gross errors on filtering results, the conventional equivalent weight function models are more suitable for the observations with the same noise level. For *Precise Point Positioning* (PPP) with multiple types of observations that have different measuring accuracy and noise levels, the filtering results obtained with conventional robust equivalent weight function models are not the best ones. For this problem, a classification robust equivalent weight function model based on the t-inspection statistics is proposed, which has better performance than the conventional equivalent weight function models in the case of no more than one gross error in a certain type of observations. However, in the case of multiple gross errors in a certain type of observations, the performance of the conventional robust Kalman filter based on the two kinds of equivalent weight function models are barely satisfactory due to the interaction between gross errors. To address this problem, an improved classification robust Kalman filtering method is further proposed in this paper. To verify and evaluate the performance of the proposed method, simulation tests were carried out based on the GPS/BDS data and their results were compared with those obtained with the conventional robust Kalman filtering method. The results show that the improved classification robust Kalman filtering method can effectively reduce the impact of multiple gross errors on the positioning results and significantly improve the positioning accuracy and reliability of PPP.

Keywords: Kalman filter, classification robust, equivalent weight function, precise point positioning.

1. Introduction

Precise Point Positioning (PPP) is a high-precision positioning solution based on precise ephemeris and clock products, using both pseudo-range and carrier phase observations [1]. Because only one dual-band receiver can achieve decimetre or centimetre level positioning accuracy, it has been widely applied in the field of surveying and mapping [2, 3]. However, the performance of PPP is not always stable in practice due to the observation data quality and gross errors in observations. In order to ensure the accuracy and reliability of the positioning results, it is generally necessary to pre-process the observation results so as to remove outliers in pseudo-range and phase-range observations [4, 5]. Nonetheless, there may still be some gross errors in

Article history: received on Sep. 03, 2018; accepted on Dec. 23, 2018; available online on Jun. 28, 2019; DOI: 10.24425/mms.2019.128354.

observations that cannot be detected. When the observations contain gross errors at a certain point in time, it will cause a jump at this point and influence the subsequent results of Kalman filter [6]. In view of this situation, a robust Kalman filter is developed to reduce the impact of gross errors on the filtering results by constructing an equivalent weight matrix according to equivalent weight function models [6–9]. In order to obtain an accurate equivalent weight matrix, there are many weight function models proposed, including Huber weight function, Danish weight function, IGG-I, IGG-II and IGG-III weight functions *etc.* [9–12]. However, the conventional robust equivalent weight function models generally use the standardized residual as the test statistics and the empirical value as the critical threshold. They are more suitable for observations with the same accuracy or noise levels and have a good robustness [9]. For PPP with multiple types of observations that have different measuring accuracy and noise levels, the filtering results based on conventional robust equivalent weight function models are not the best ones [8]. The reason is that the random characteristics of different types of observations are different and their a posteriori residuals are different as well. The standardized residuals are normalized values of a posteriori residuals, which is related to the a priori weights of the observations. When the a priori weights of different types of observations are not precise, the distributions of standardized residuals of different types of observations will not be the same. Thus, the equivalent weight matrix calculated by the conventional robust equivalent weight function models will not be accurate [8]. On the other hand, choosing an empirical value as the detection threshold for the equivalent weight model may cause a significant risk that the weights of some healthy observations are reduced or the observations with gross errors cannot be detected at a certain point in time [13, 14]. To overcome those problems of the robust Kalman filter based on the conventional robust equivalent weight function models for PPP, a classification robust Kalman filter based on the classification robust weight function model is proposed [15]. The new robust weight function model using the t-inspection statistics, and the equivalent weight matrix of different types of observations are calculated separately. The robust Kalman filter based on the classification robust weight function model has a better performance than that based on the conventional robust weight function models in the case of no more than one gross error in a certain type of observation. However, in the case of multiple gross errors in a certain type of observation, the performance of the robust Kalman filter based on the two kinds of robust weight function models is barely satisfactory. To address this problem, an improved classification robust Kalman filtering method is further proposed in this paper. Simulation tests were performed based on the GPS/BDS data to verify the effectiveness of the proposed method.

In the following sections, we first introduce the basic models of PPP and robust Kalman filtering estimation, then give the conventional robust weight function model and the classification robust weight function model, and introduce an improved classification robust Kalman filter method. Finally, we analyse the performance and problems of the conventional and classification robust weight function models, and verify the effectiveness and evaluate the performance of the improved classification robust Kalman filtering.

2. Basic models of precise point positioning

There are many observation models developed for PPP, including the *ionosphere-free* (IF) combination model, Uofc model, un-combined model [1, 16–18]. Because the IF combination model can eliminate nearly all of the ionospheric propagation delays by a combination of dual-frequency data with a simple model, it has been widely used as the observation model for PPP [19]. Moreover, in order to obtain the optimal solutions, Kalman filter is usually used to estimate the

unknown state parameters, such as position, velocity, receiver clock bias [5]. The IF combination observation model and the EKF (*extended Kalman filter*)-based parameter estimation method for PPP are described in detail below.

2.1. Ionospheric-free combination observation model

In *Precise Point Positioning*, where dual-band code pseudo-range and phase-range observations in the ionosphere-free combination are generally used, a simplified IF combination observation model is as follows [1, 2]:

$$P_{\mathrm{IF}} = \rho + c\left(dt_r - dt^s\right) + T + \varepsilon_{P_{\mathrm{IF}}}, \tag{1}$$

$$\Phi_{\mathrm{IF}} = \rho + c\left(dt_r - dt^s\right) + T + \lambda_{\mathrm{IF}} N_{\mathrm{IF}} + \varepsilon_{\Phi_{\mathrm{IF}}}, \tag{2}$$

where P_{IF} is the IF combination code pseudo-range observation and Φ_{IF} is the corresponding IF combination phase-range observation; ρ is the geometric distance between the receiver and the satellite; c is the vacuum speed of light; dt_r and dt^s are the receiver and satellite clock offsets; T is the tropospheric delay; λ_{IF} is the IF linear combination carrier wavelength and N_{IF} is the corresponding float carrier-phase bias; $\varepsilon_{P_{\mathrm{IF}}}$ and $\varepsilon_{\Phi_{\mathrm{IF}}}$ are the code noises of pseudo-range and phase-range observations in the IF linear combination, respectively.

According to the observation model, there are at least two types of observations in PPP, including pseudo-range and phase-range observations. Generally, for the GPS, the precision values of P code and C/A code pseudo-range are about 0.3 m and 3 m, and the precision value of phase-range is about 1~2 mm [19]. Therefore, the phase-range observation has a higher accuracy than the pseudo-range observation.

2.2. Parameter estimation based on extended Kalman filter

According to (1) and (2), the observation equation is a non-linear function that is related to the receiver's three-dimensional position, so the measurement model for PPP is non-linear. The state and measurement model for Kalman filter can be described by:

$$\boldsymbol{y}_k = \boldsymbol{h}(\boldsymbol{x}_k) + \boldsymbol{v}_k, \tag{3}$$

$$\boldsymbol{x}_k = \boldsymbol{F}_{k,k-1}\boldsymbol{x}_{k-1} + \boldsymbol{w}_k, \tag{4}$$

where $\boldsymbol{h}(\boldsymbol{x})$ is an observation model function vector; $\boldsymbol{F}_{k,k-1}$ is a transition matrix; $\boldsymbol{w}_k$ and $\boldsymbol{v}_k$ are usually uncorrelated white noise vectors of the system and the measurement respectively, and the corresponding covariance matrix is obtained as:

$$\mathrm{cov}(\boldsymbol{w}_k, \boldsymbol{w}_k) = \boldsymbol{Q}_k, \qquad \mathrm{cov}(\boldsymbol{v}_k, \boldsymbol{v}_k) = \boldsymbol{R}_k, \tag{5}$$

where $\boldsymbol{Q}_k$ is a system noise covariance matrix; $\boldsymbol{R}_k$ is a measurement noise covariance matrix. The unknown state vector $\boldsymbol{x}$ for the PPP is set as:

$$\boldsymbol{x} = \left(\boldsymbol{r}, dt_r, Z_r, N_{\mathrm{IF}}^1, N_{\mathrm{IF}}^2, \ldots, N_{\mathrm{IF}}^n\right)^T, \tag{6}$$

and the observation vector $\boldsymbol{y}$ is defined by the IF linear combination pseudo-range and phase-range observations as:

$$\boldsymbol{y} = \left(P_{\mathrm{IF}}^1, P_{\mathrm{IF}}^2, \ldots, P_{\mathrm{IF}}^n, \Phi_{\mathrm{IF}}^1, \Phi_{\mathrm{IF}}^2, \ldots, \Phi_{\mathrm{IF}}^n\right)^T, \tag{7}$$

where $\boldsymbol{r} = (x, y, z)$ are the receiver's coordinates and velocity in the *Earth-Centred-Earth-Fixed* (ECEF) frame; Z_r is the *zenith total delay* (ZTD).

By using EKF, the state vector $\hat{\boldsymbol{x}}$ for unknown model parameters and its covariance matrix $\boldsymbol{P}_{\hat{x}}$ can be estimated with the measurement vector $\boldsymbol{y}_{\mathrm{k}}$ at an epoch t_k by [21]:

$$\hat{\boldsymbol{x}}_k = \bar{\boldsymbol{x}}_k + \boldsymbol{K}_k \left(\boldsymbol{y}_k - h(\hat{\boldsymbol{x}}_k)\right), \tag{8}$$

$$\boldsymbol{P}_{\hat{\boldsymbol{x}}_k} = (\boldsymbol{I} - \boldsymbol{K}_k \boldsymbol{H}_k)\boldsymbol{P}_{\bar{\boldsymbol{x}}_k}, \tag{9}$$

$$\boldsymbol{K}_k = \boldsymbol{P}_{\bar{\boldsymbol{x}}_k} \boldsymbol{H}_k^T \left(\boldsymbol{H}_k \boldsymbol{P}_{\bar{\boldsymbol{x}}_k} \boldsymbol{H}_k^T + \boldsymbol{R}_k\right)^{-1}, \tag{10}$$

$$\bar{\boldsymbol{x}}_k = \boldsymbol{F}_{k,k-1} \hat{\boldsymbol{x}}_{k-1}, \tag{11}$$

$$\boldsymbol{P}_{\bar{\boldsymbol{x}}_k} = \boldsymbol{F}_{k,k-1} \boldsymbol{P}_{\hat{\boldsymbol{x}}_{k-1}} \boldsymbol{F}_{k,k-1}^T + \boldsymbol{Q}_{k,k-1}, \tag{12}$$

where $\bar{\boldsymbol{x}}_k$ and $\boldsymbol{P}_{\bar{\boldsymbol{x}}_k}$ are the time-propagated state estimates and covariance; $\boldsymbol{R}_k$ is the measurement noise covariance matrix; $\boldsymbol{H}_k = \partial \boldsymbol{h}(\boldsymbol{x})/\partial \boldsymbol{x}|_{\boldsymbol{x}=\hat{\boldsymbol{x}}}$ is the matrix of partial derivatives; $\boldsymbol{K}_k$ is the Kalman gain matrix.

3. Robust Kalman filter

For the standard Kalman filter, the results of state estimation are extremely sensitive to the gross errors in observations, so that it shows its instability and even divergence. According to (8), when the measurement vector $\boldsymbol{y}_k$ contains gross errors, the state estimation will be influenced by the gain matrix $\boldsymbol{K}_k$. In order to reduce the impact of gross errors on filtering results, the robust estimation is developed by constructing an equivalent weight matrix of observations [6–9].

According to the theory of robust estimation, the recursive solution of state parameters calculated by (8) can be rewritten as [9]:

$$\hat{\boldsymbol{x}}_k = \bar{\boldsymbol{x}}_k + \overline{\boldsymbol{K}}_k \left(\boldsymbol{y}_k - h(\bar{\boldsymbol{x}}_k)\right), \tag{13}$$

where $\overline{\boldsymbol{K}}_k$ is the Kalman gain matrix based on the equivalent weight matrix of observations, *i.e.*:

$$\overline{\boldsymbol{K}}_k = \boldsymbol{P}_{\bar{\boldsymbol{x}}_k} \boldsymbol{H}_k^T \left(\boldsymbol{H}_k \boldsymbol{P}_{\bar{\boldsymbol{x}}_k} \boldsymbol{H}_k^T + \overline{\boldsymbol{R}}_k\right)^{-1}, \tag{14}$$

$\overline{\boldsymbol{R}}_k$ is the equivalent covariance matrix of observations, which is usually obtained by multiplying $\boldsymbol{R}_k$ by a weight matrix $\overline{\boldsymbol{P}}$ as follows:

$$\overline{\boldsymbol{R}}_k = \boldsymbol{R}_k \cdot \overline{\boldsymbol{P}}. \tag{15}$$

In the above equations, $\overline{\boldsymbol{P}}$ is calculated by the equivalent weight function model. In the observation-independent case, $\overline{\boldsymbol{P}}$ is a diagonal matrix. The variances of pseudo-range and phase-range observations are usually determined by the stochastic model based on elevation angle [22]:

$$\sigma^2 = F^s R_r^2 \left(a_\sigma^2 + b_\sigma^2 / \sin E^2\right) + \sigma_{eph}^2 + \sigma_{ion}^2 + \sigma_{trop}^2 + \sigma_{bias}^2, \tag{16}$$

where F^s is a satellite system error factor (GPS:1, BDS:2); R_r is a code/carrier-phase error ratio (GPS, BDS MEO and IGSO:100, BDS GEO: 300); the parameters a_σ and b_σ are carrier-phase error factors, which are usually set to 0.003; E is a satellite elevation angle; $\sigma_{eph}, \sigma_{ion}, \sigma_{trop}$ and σ_{bias} are standard deviation of ephemeris and clock, ionosphere correction model, troposphere correction model and code bias errors, respectively. The covariance matrix is constructed by:

$$\boldsymbol{R}_k = \mathrm{diag}\left\{\boldsymbol{\sigma}_{\boldsymbol{P}_{\mathrm{IF}}}^2,\ \boldsymbol{\sigma}_{\boldsymbol{\Phi}_{\mathrm{IF}}}^2\right\}, \tag{17}$$

where $\boldsymbol{\sigma}_{\boldsymbol{P}_{\mathrm{IF}}}^2$ and $\boldsymbol{\sigma}_{\boldsymbol{\Phi}_{\mathrm{IF}}}^2$ are covariance matrices of the IF combination pseudo-range and phase-range observations and they are diagonal matrices.

3.1. Conventional robust equivalent weight function model

In order to obtain the equivalent weight matrix $\overline{\boldsymbol{P}}$, many equivalent weight function models have been developed, including Huber weight function, Danish weight function, IGG-III weight function [9–12]. In general, IGG-III is a good choice to use for constructing the equivalent weight matrix and the function model is expressed as follows [9]:

$$P_i = \begin{cases} 1 & |\overline{v}_i| \le k_0 \\ \dfrac{|\overline{v}_i|}{k_0}\left(\dfrac{k_1 - k_0}{k_1 - |\overline{v}_i|}\right)^2 & k_0 < |\overline{v}_i| \le k_1 \\ \infty & |\overline{v}_i| > k_1 \end{cases}, \tag{18}$$

where k_0 and k_1 are constants which are found to have the values $k_0 = 1.0\sim2.0$, $k_1 = 3.0\sim8.0$. P_i is the diagonal element of the weight matrix $\overline{\boldsymbol{P}}$. $\overline{v}_i$ is the standardized residual corresponding to the measurement residual v_i of the observation y_i, which can be calculated by the following equation:

$$\overline{v}_i = v_i / \sqrt{\hat{\sigma}_0^2 Q_{v_i v_i}}\,, \tag{19}$$

$Q_{v_i v_i}$ is the diagonal element of the covariance matrix $\boldsymbol{Q}_v$ of measurement residuals $\boldsymbol{v}$ and

$$\boldsymbol{Q}_v = \boldsymbol{R}_k - \boldsymbol{H}_k \boldsymbol{P}_{\hat{\boldsymbol{x}}_k} \boldsymbol{H}_k^T\,, \tag{20}$$

$\hat{\sigma}_0^2$ is the estimate of unit weight variance. According to the theory of generalized least squares, it can be calculated by the following equation [23]:

$$\hat{\sigma}_0^2 = \frac{\boldsymbol{v}^T \boldsymbol{P} \boldsymbol{v} + \boldsymbol{v}_{\boldsymbol{x}}^T \boldsymbol{P}_{\hat{\boldsymbol{x}}}^{-1} \boldsymbol{v}_{\boldsymbol{x}}}{n} = \frac{\boldsymbol{\xi}^T \boldsymbol{Q}_{\boldsymbol{\xi}}^{-1} \boldsymbol{\xi}}{n}\,, \tag{21}$$

where

$$\boldsymbol{\xi} = \boldsymbol{y}_k - h\left(\overline{\boldsymbol{x}}_k\right), \tag{22}$$

$$\boldsymbol{Q}_{\boldsymbol{\xi}} = \boldsymbol{R}_k + \boldsymbol{H}_k \boldsymbol{P}_{\overline{\boldsymbol{x}}_k} \boldsymbol{H}_k^T\,, \tag{23}$$

$\boldsymbol{v}_x$ and $\boldsymbol{\xi}$ are the state residual vector and the predicted residual vector (innovation), respectively; $\boldsymbol{Q}_{\boldsymbol{\xi}}$ is the covariance matrix of $\boldsymbol{\xi}$; n is the number of measurements.

The conventional equivalent weight function model described by (18) is constructed by the standardized residual statistics and the critical values are often established by experience. It has a good performance for observations with the same accuracy and has been verified and widely used. However, its robustness is not optimal for GNSS PPP with multiple types of observations with different measuring accuracy [11]. That is because the conventional robust equivalent weight function model suggests that all types of observations have the same unit weight variance, although they are actually different. Thus, the distributions of the standardized residuals calculated by (19) for different types of observations will be different and critically may cause a significant risk, resulting in a decrease in robustness and influencing the positioning accuracy of PPP. Those problems will be illustrated in simulation tests and analysis of their results.

3.2. Classification robust equivalent weight function model

Although the distribution of standardized residuals for different types of observations vary, the distribution of the same type of observations is the same and follows the normal distribution

in the case of absence of gross errors in observations. So, the equivalent weight matrices for each type of observation can be constructed based on the standardized residuals separately. According to this idea, a t-inspection criterion-based classification robust equivalent weight function model is proposed which adopts the t-inspection statistics, and the equivalent weight function model is described as follows [15]:

$$P_j^i = \begin{cases} 1 & T_j^i \le t_0(a_0, \tau) \\ \dfrac{T_j^i}{t_0}\left(\dfrac{t_1 - t_0}{t_1 - T_j^i}\right)^2 & t_0(a_0, \tau) < T_j^i \le t_1(a_1, \tau) \\ \infty & T_j^i > t_1(a_1, \tau) \end{cases}, \tag{24}$$

where the superscript i, $i = 1, 2, \ldots, N$, indicates the type of observation, N is the number of types of observations (for a single GNSS PPP there are two types of observations, including pseudo-range and phase-range ones, $N = 2$; for multiple GNSS PPP, there are more than two types, *i.e.* GPS/BDS PPP, $N = 4$). t_0 and t_1 are t-inspection coefficients at significance levels a_0 and a_1 with a degree of freedom $\tau = n^i - 1$. T_j^i is the t-inspection statistics of the i-th type of observation, which is calculated by the following equation [13, 24]:

$$T_j^i = \frac{\left| \overline{v}_j^i - \dfrac{1}{n^i - 1} \displaystyle\sum_{\substack{k=1 \\ k \ne j}}^{n^i} \overline{v}_k^i \right|}{\sqrt{\dfrac{1}{n^i - 2} \displaystyle\sum_{\substack{k=1 \\ k \ne j}}^{n^i} \left(\overline{v}_k^i - \dfrac{1}{n^i - 1} \displaystyle\sum_{\substack{l=1 \\ l \ne k}}^{n^i} \overline{v}_l^i \right)^2}}, \tag{25}$$

where $\overline{v}_j^i$ is the standardized residual of the j-th measurement of the i-th type of observation. n^i is the number of measurements of the i-th type of observation. The total weight matrix $\overline{\boldsymbol{P}}$ can be constructed by the sub-weight matrix $\overline{\boldsymbol{P}}^i$ ($i = 1, 2, \ldots, N$):

$$\overline{\boldsymbol{P}} = \operatorname{diag}\left\{ \overline{\boldsymbol{P}}^1, \overline{\boldsymbol{P}}^2, \ldots, \overline{\boldsymbol{P}}^N \right\}, \tag{26}$$

where $\operatorname{diag}\{\cdot\}$ indicates a diagonal matrix. Because the t-inspection statistics reflects the dispersion degree of measurement residuals among one certain type of observations, it will not be affected by the residuals of other types of observations and has a higher sensitivity to gross errors in each type of observations.

3.3. Improved classification robust Kalman filtering algorithm

The conventional robust Kalman filter is based on the iteration method with variable weights determined by the equivalent weight function models. It has a good robustness in the presence of no more than one gross error. However, for the presence of multiple gross errors in a certain type of observation, the performance of robust Kalman filter based on the conventional and classification robust equivalent weight function models will be reduced or even lead to the failure of robustness due to the interaction of gross errors. In order to improve the robustness of Kalman filter in the case of multiple gross errors in a certain type of observation for PPP, an improved classification

robust Kalman filtering algorithm is proposed. In the improved method, for a certain type of observation with gross errors, only one observation that is most likely to contain a gross error is weighted when the robust weighting is performed to avoid a wrong weighting for the healthy observations caused by the interactions of multiple gross errors, while for the types of observations which do not contain gross errors, the classification robust equivalent weight function model is used to calculate the equivalent weights of observations. Because the *weighted sum squared of measurement residuals* (WSSR) has a chi-square distribution without considering the dynamic model error, the chi-square test can be used to detect the faults globally and the normalized test statistics for each type of observations is as follows [25]:

$$r^i = \frac{\boldsymbol{v}^{iT}\overline{\boldsymbol{R}}^{i-1}\boldsymbol{v}^i}{\sigma_0^{i\,2}} \sim \chi^2_{1-a,\upsilon} \qquad (\upsilon = n-m, \quad i = 1, 2, \ldots, N), \tag{27}$$

where σ_0^2 is the a priori variance factor; υ is the number of degrees of freedom which is equal to the difference between the number of observations n and the number of estimated parameters m. It is determined whether there are gross errors in a certain type of observation by comparing the test statistics r^i and the threshold $T\,h^i$ calculated at the significance level a.

A flowchart of the improved classification robust Kalman filtering algorithm is shown in Fig. 1.

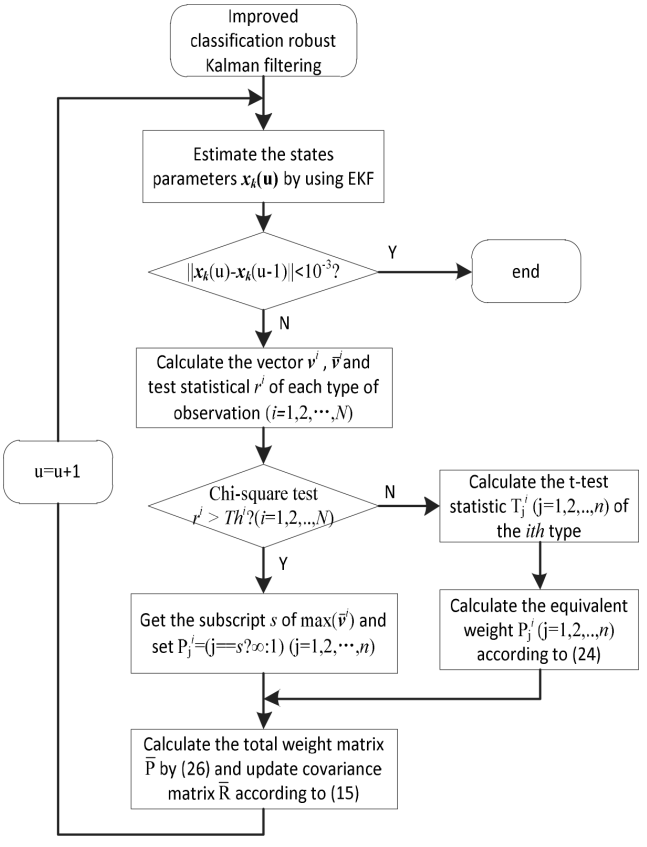

Fig. 1. A flowchart of the improved classification robust Kalman filtering algorithm for PPP.

It comprises the following steps:

Step 1: Estimate the state parameters $x_k(u)$ by using EKF according to (8)~(12).

Step 2: Perform the Chi-square test for each type of observations. Calculate the measurement residual $\boldsymbol{v}^i$, the standardized residual $\overline{\boldsymbol{v}}^i$ and the test statistics r^i $(i = 1, 2, \ldots, N)$ for each type of observations. If $r^i > Th^i$, it indicates that there are some gross errors in the i-th type of observation.

Step 3: Calculate the total equivalent weight matrix $\overline{\boldsymbol{P}}$ and update the covariance matrix $\overline{\boldsymbol{R}}$. First, the sub-weight equivalent weight matrix $\overline{\boldsymbol{P}}^i$ $(i = 1, 2, \ldots, N)$ is calculated. In step 2, if $r^i > Th^i$, the sub-weight matrix $\overline{\boldsymbol{P}}^i$ for the i-th type of observation is calculated by the following function model:

$$P_j^i = \begin{cases} 1 & j \neq s \\ \infty & j = s \end{cases}, \tag{28}$$

where s is the subscript of the max value of $\overline{\boldsymbol{v}}^i$. If $r^i \leq Th^i$, calculate the sub-weight matrix $\overline{\boldsymbol{P}}^i$ for the i-th type of observation according to (24). Then, the total equivalent weight matrix is constructed according to (26), and the covariance matrix is updated according to (15).

Step 4: Repeat steps 1 to 3 until the change in the state parameter satisfies the following condition:

$$\|x_k(u) - x_k(u-1)\| < 10^{-3}, \qquad x_k(0) = \{0\}, \tag{29}$$

where u is the number of times of performing the robust filtering at time k-th, and the initial value of state vector $x_k(0)$ is set to zeros.

4. Tests and analysis

To verify the effectiveness of the classification robust equivalent weight function model and to assess the performance of the improved classification robust Kalman filtering method for PPP, simulation tests were carried out with GPS/BDS data. The test data set was obtained from *International GNSS Service* (IGS) Multi-GNSS Experiment data centre at JFNG reference station on May 30, 2018. Fig. 2 shows the number of the available satellites and GDOP of GPS, BDS and

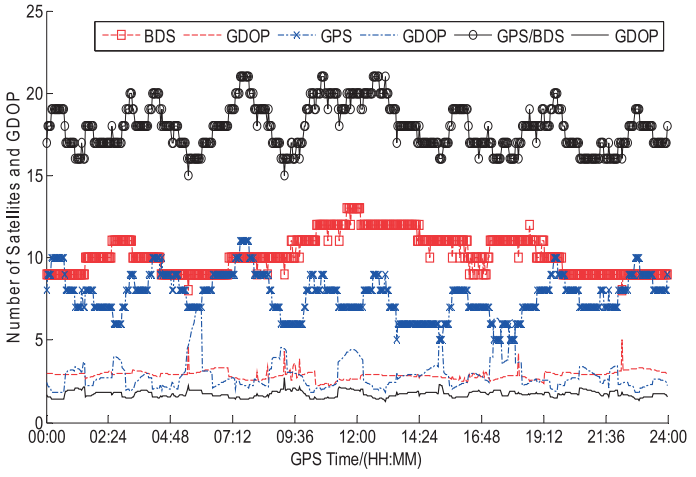

Fig. 2. The number of available satellites and GDOP at JFNG station on May 30, 2018 (cut angle 15°).

GPS/BDS. The products such as precise satellite orbits (15 min) and clocks (30 s) used in PPP were provided by IGS data centre of Wuhan University [26]. In the following sections, we first discuss the conventional and classification robust equivalent weight function models, verify the effectiveness of the classification robust function model assuming that no more than one gross error in a certain type of observation exists, and further analyse the problems of the conventional robust Kalman filtering algorithm based on the two kinds of equivalent weight function models in the case of multiple gross errors in a certain type of observation. Finally, we verify and evaluate the performance of the improved classification robust Kalman filtering algorithm.

4.1. Analysis of conventional and classification robust equivalent weight function models

In order to analyse the advantages and disadvantages of the conventional and classification robust equivalent weight function models, the following five cases were studied. In each case, an *extended Kalman filter* (EKF), a robust Kalman filter with the conventional *robust equivalent weight function* model (RKF), and a robust Kalman filter with the *classification robust equivalent weight function* model (CRKF) were used to calculate the positioning results of GPS PPP. The *root-mean-square* (RMS) values of positioning errors were counted in order to analyse the performance of different filtering methods.

Case 1: No gross errors in pseudo-range and phase-range observations.

Case 2: Gross errors with values of 100 m were added to pseudo-range observations for a random satellite from 5:00 to 6:00 (one gross error only in each pseudo-range observation).

Case 3: Gross errors with values of 1 m were added to phase-range observations for a random satellite from 5:00 to 6:00 (one gross error only in each phase-range observation).

Case 4: Gross errors with values of 100 m and 1 m were respectively added to pseudo-range and phase-range observations for a random satellite from 5:00 to 6:00 (one gross error in each of pseudo-range and phase-range observations).

Case 5: Gross errors with values of 100 m and 1 m were respectively added to pseudo-range and phase-range observations for two random satellites from 5:00 to 6:00 (two gross errors in each of pseudo-range and phase-range observations).

Figure 3 shows the standardized residual distribution of pseudo-range and phase-range observations in the absence of gross errors. The results show that the standard variance of pseudo-range standardized residuals is equal to 1.25, while the standard variance of phase-range standardized residuals is equal to 0.67. Obviously, they have different distribution characteristics. According to the distribution characteristics of standardized residuals, k0 = 1.5 and k1 = 3.5 were selected as the critical values for the conventional robust equivalent weight function model. For the clas-

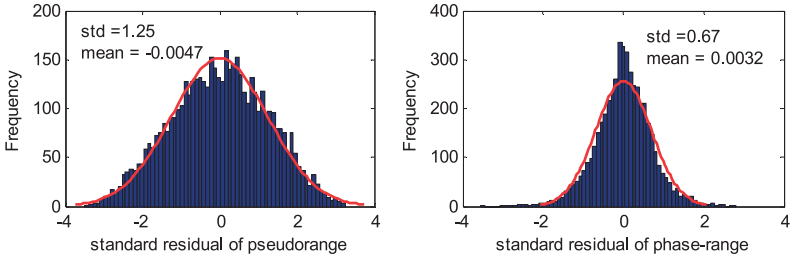

Fig. 3. Distributions of standardized residuals for pseudo-range and phase-range observations in the absence of gross errors.

sification robust equivalent weight function model, the thresholds t0 and t1 were obtained from the t-inspection coefficient table with the significance levels a0 = 0.1 and a1 = 0.01.

Figures 4, 5 and 6 show sequences of the standardized residuals and t-inspection statistics for phase-range and pseudo-range observations for cases 2, 3 and 4 that assume only one gross error in a certain type of observation. Fig. 7 shows sequences of the standardized residuals and t-inspection statistics for phase-range and pseudo-range observations for case 5 that the presence of multiple gross errors in a certain type of observation is assumed. The RMS values of positioning errors of GPS PPP with EKF, RKF and CRKF for the different cases are listed in Table 1.

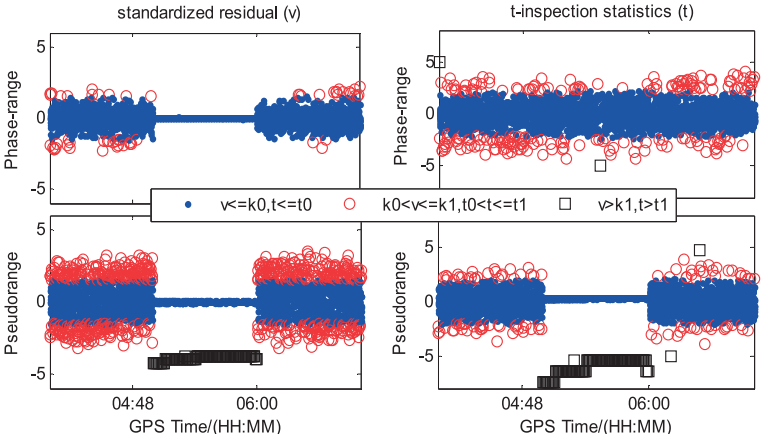

Fig. 4. Sequences of standardized residuals and t-inspection statistics for pseudo-range and phase-range observations in case 2.

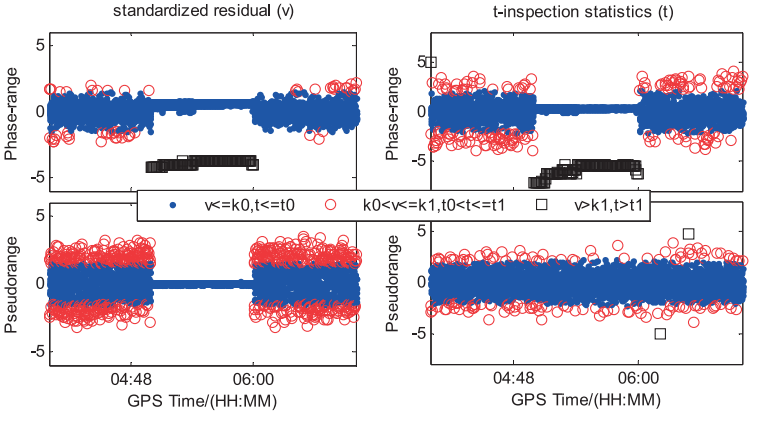

Fig. 5. Sequences of standardized residuals and t-inspection statistics for pseudo-range and phase-range observations in case 3.

It can be seen from Figs. 4 to 6 that the conventional robust equivalent weight function model based on standardized residual statistics can detect outliers in the case of existing gross errors only in a certain type of observation, but it cannot detect the outliers in pseudo-range observations in the case of existing a gross error in each of pseudo-range and phase-range observations. Because the gross errors in phase-range observations have a greater contribution to the measurement

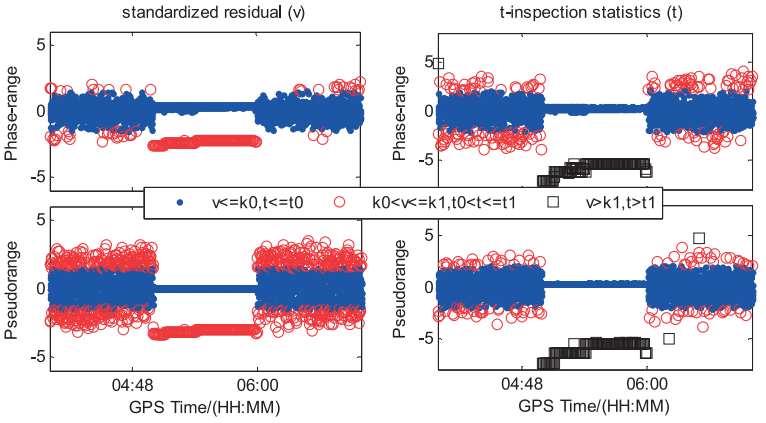

Fig. 6. Sequences of standardized residuals and t-inspection statistics for pseudo-range and phase-range observations in case 4.

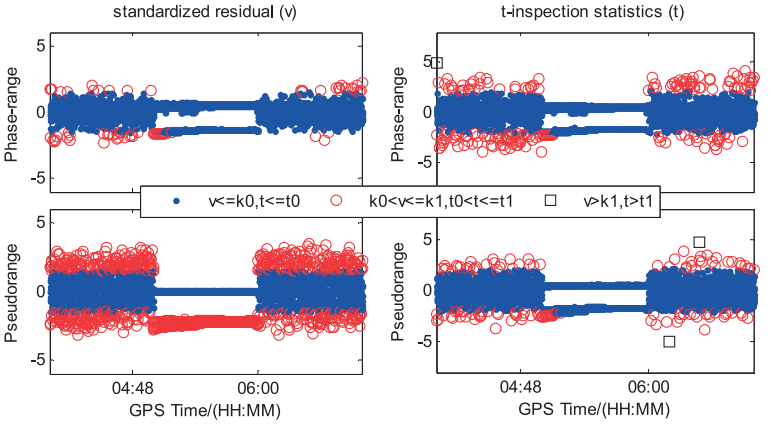

Fig. 7. Sequences of standardized residuals and t-inspection statistics for pseudo-range and phase-range observations in case 5.

Table 1. RMS values of positioning errors of GPS PPP with EKF, RKF and CRKF for different cases.

Gross error cases	EKF (RMS/cm)			RKF (RMS/cm)			CRKF (RMS/cm)		
	East	North	Up	East	North	Up	East	North	Up
Case 1	0.24	0.69	0.45	0.23	0.65	0.41	0.26	0.48	0.45
Case 2	0.85	2.68	2.58	0.23	0.87	0.55	0.27	0.49	0.45
Case 3	3.97	2.87	5.76	0.25	0.57	0.46	0.26	0.48	0.44
Case 4	8.43	6.51	8.09	4.54	1.79	3.89	0.27	0.50	0.44
Case 5	13.42	11.56	9.93	11.92	13.94	8.38	13.43	11.95	7.75

residuals, the standardized residuals of pseudo-range observations with gross errors are below the critical value. However, the t-inspection statistics of phase-range and pseudo-range observations with gross errors from 5:00 to 6:00 are all greater than the threshold, so the outliers can be

detected by the classification robust equivalent weight function model not only in the case of gross errors in a certain type of observation, but also in the case of gross errors in both types. In addition, based on the comparison of the positioning errors of EKF for different cases given in Table 1, the performance of PPP will be reduced when the observations contain gross errors, and the impact of gross errors in phase-range observations on the positioning results is more obvious than that of gross errors in pseudo-range observations. Moreover, based on the comparison of the positioning errors of EKF, RKF and CRKF for cases 2, 3 and 4 given in Table 1, both RKF and CRKF methods can reduce the impact of gross errors on the positioning results in cases 2 and 3 that assume one gross error only in a certain type of observation, and they have almost the same performance. However, in case 3 assuming one gross error in each of pseudo-range and phase-range observations, the CRKF method outperforms the RKF method. In fact, the RKF method just eliminates the effect of gross errors in phase-range observations on the positioning results, while the CRKF method can eliminate the effect of gross errors in both types of observations at the same time. So the classification robust equivalent weight function model is more effective than the conventional robust equivalent weight function model for PPP in the case of no more than one gross error existing in a certain type of observation.

However, the conventional robust Kalman filter based on the two kinds of robust equivalent weight function models (RKF and CRKF) may be subjected to the risk of low robustness or even failing a robust estimation in the case of multiple gross errors in a certain type of observation. Case 5 illustrates this situation. As can be seen from Fig. 7, the standardized residual and t-inspection statistics cannot detect gross errors in pseudo-range and phase-range observations, and the positioning results in Table 1 show that neither RKF nor CRKF method has a good robustness.

4.2. Performance evaluation of improved classification robust Kalman filtering algorithm

To verify the effectiveness and evaluate the performance of the improved classification robust Kalman filter method, the following five schemes were designed. In schemes 2, 3, 4 and 5, gross errors with values of 100 m and 1 m were added to pseudo-range and phase-range observations of two random satellites from 5:00 to 6:00.

Scheme 1: Standard Kalman filtering for GPS/BDS PPP with no gross errors in observations (EKF with no gross errors)

Scheme 2: Standard Kalman filtering for GPS/BDS PPP with simulated gross errors (EKF with gross errors).

Scheme 3: Conventional robust Kalman filtering for GPS/BDS PPP with simulated gross errors and the critical values k0 = 1.5, k1 = 3.5 (RKF).

Scheme 4: Classification robust Kalman filtering for GPS/BDS PPP with simulated gross errors and the significant levels a0 = 0.1, a1 = 0.01 (CRKF).

Scheme 5: Improved classification robust Kalman filtering for GPS/BDS PPP with simulated gross errors and the significant levels a0 = 0.1, a1 =0.01 (ICRKF).

Table 2. RMS values of positioning errors for different filtering schemes.

Items		**EKF (no gross errors)**	**EKF**	**RKF**	**CRKF**	**ICRKF**
RMS/cm	**East**	0.162	9.889	6.067	9.350	0.421
	North	0.409	22.16	10.96	20.17	0.413
	Up	0.306	11.90	4.118	10.75	0.252

Figures 8, 9 and 10 show the positioning errors of five schemes in the directions of *East* (E), *North* (N) and *Up* (U). The RMS values of positioning errors are shown in Table 2. It is obvious that RKF and CRKF all have low robustness. In particular, CRKF can hardly reduce the influence of gross errors in the case of multiple gross errors in a certain type of observation. By comparing the position error curve and positioning accuracy of the five schemes, we conclude that ICRKF has the best performance, which can reduce the impact of multiple gross errors on the positioning results and significantly improve the positioning accuracy.

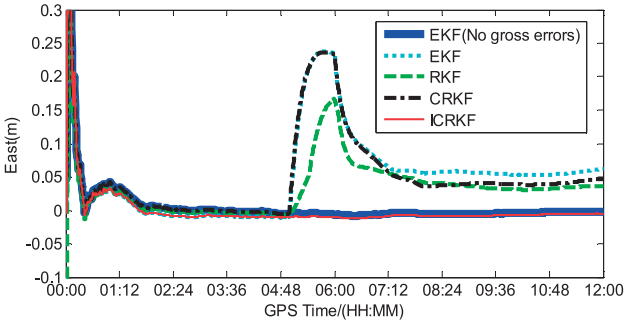

Fig. 8. Positioning error sequences in East direction for five schemes.

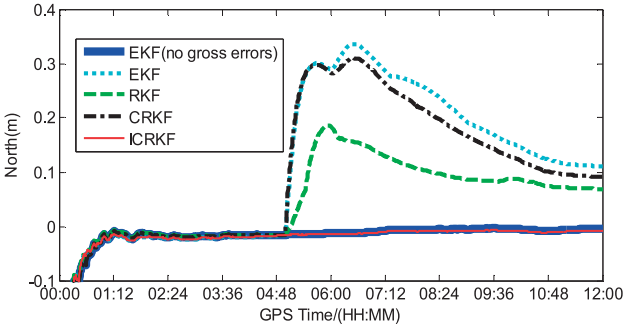

Fig. 9. Positioning error sequences in North direction for five schemes.

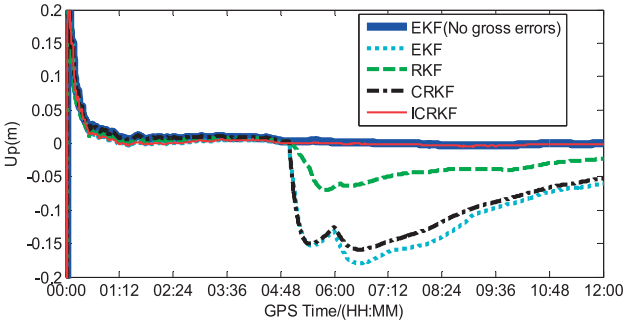

Fig. 10. Positioning error sequences in Up direction for five schemes.

5. Conclusions

The conventional robust equivalent weight function model has a good robustness for observations with the same error distribution. However, the performance is not optimal regarding multiple types of observations with different accuracy. Because the distributions of residuals are different due to the different error distributions of various types of observations, the conventional robust equivalent weight function models may lead to the overall reduction of weights in a certain type of observation without gross errors thus affecting the filtering results. The classification robust equivalent weight function model constructs a weight matrix for each type of observations respectively based on the t-inspection statistics, which can reduce the mutual influence between residuals of different types of observations and improve the recognition rate of gross errors. However, the robust Kalman filter based on the classification robust equivalent weight function model has a good performance only if there is less than one gross error in a certain type of observations. In the presence of multiple gross errors in a certain type of observations, the conventional robust Kalman filter based on the two kinds of equivalent weight function models is subjected to the risk of low robustness and failing to provide a robust estimation. In this paper, an improved classification robust Kalman filtering algorithm is proposed to improve the robustness in the presence of multiple gross errors in a certain type of observations. The results show that the proposed method can effectively reduce the impact of multiple gross errors on the positioning results and significantly improve the accuracy and stability of PPP.

Acknowledgements

This project was supported by the National Natural Science Foundation of China (Grants No. 41874034, 41574024), the National Science and Technology Major Project of the National Key R&D Program of China (Grant No.2016YFB0502102), the Beijing Natural Science Foundation (Grant No. 4162035), and the Aeronautical Science Foundation of China (Grant No. 2016ZC51024), and the Academic Excellence Foundation of BUAA for PhD Students.

References

[1] Kouba, J., Héroux, P. (2001). Precise point positioning using IGS orbit and clock products. *GPS solutions*, 5(2), 12–28.

[2] Zumberge, J.F., Heflin, M.B., Jefferson, D.C. (1997). Precise point positioning for the efficient and robust analysis of GPS data from large networks. *Journal of Geophysical Research Solid Earth*, 102(B3), 5005–5017.

[3] Wang, M., Chai, H.Z., Li, Y. (2017). Performance analysis of BDS/GPS precise point positioning with undifferenced ambiguity resolution. *Advances in Space Research*, 60(12), 2581–2595.

[4] Subirana, S.J., Juan, Z.J.M., Hernández-Pajares, H. (2013). GNSS Data Processing, I. *Fundamentals and Algorithms*. 1nd ed. Netherlands: ESA Communications.

[5] Kouba J., Lahaye, F., Tétreault, P. (2017). Precise Point Positioning. Teunissen P.J., Montenbruck O., eds. *Springer Handbook of Global Navigation Satellite Systems*. Springer Handbooks. Springer, Cham, 723–751.

[6] Li, Z.K., Yao, Y.F., Wang, J., Gao, J.X. (2017). Application of Improved Robust Kalman Filter in Data Fusion for PPP/INS Tightly Coupled Positioning System. *Metrol. Meas. Syst.*, 24(2), 289–301.

[7] Guo, F., Zhang, X.H. (2014). Adaptive robust Kalman filtering for precise point positioning. *Measurement Science and Technology*, 25(10), 105–113.

[8] Wang, Y., Zhang, C.D., Hu, X.G., Song, Y.Z., Ma, S.L. (2016). Robust Kalman filter based on different satellite types and it's application in GPS/BDS precise point positioning. *Journal of Chinese Inertial Technology*, 24(6), 769–779.

[9] Yang, Y.X. He, H.B., Xu, G. (2001). Adaptively robust filtering for kinematic geodetic positioning. *Journal of Geodesy*, 75(1), 109–116.

[10] Yang, Y.X., Wu, F.M. (2006). Modified equivalent weight function with variable criterion for robust estimation. *Journal of Zhengzhou institute of Surveying and Mapping*, 23(5), 137–320.

[11] Lin, G.L., Liu, L., Cai, C., Li, J.Y, Hang, L. (2015). An improved Two-Step M estimation method based on the Danish method. *Journal of Geodesy and Geodynamics*, 35(2), 235–238.

[12] Krarup, T., Juhl, J., Kubik, K. (1980). Gotterdammerlung over least squares adjustment. 14th Congress ISP Hamburg, 36–38.

[13] Yang, Y.X., Xu, J.Y. (2016). GNSS receiver autonomous integrity monitoring (RAIM) algorithm based on robust estimation. *Geodesy and Geodynamics*, 7(2), 117–123.

[14] Huang, Y.L., Zhang, Y.G., Wu, Z.M., Li, N., Chamber, J. (2017). A novel robust Student's based Kalman filter. *IEEE Transactions on Aerospace and Electronic Systems*, 53(3), 1545–1554.

[15] Zhang, Q.Q., Zhao, L.D., Zhao, L., Zhou, J.H. (2018). An improved robust adaptive Kalman Filter for GNSS Precise Point Positioning. *IEEE Sensors Journal*, 18(10), 4176–4186.

[16] Gao, Y., Shen, X. (2001). Improving ambiguity convergence in carrier phase-based precise point positioning. *Proceeding of ION GPS 2001*, Salt Lake City, UT, 1532–1539.

[17] Zhang, B.C., Ou, J.K., Yuan, Y.B., Zhong, S.M. (2010). Precise point positioning algorithm based on original dual-frequency GPS code and carrier-phase observations and its application. *Acta Geodaetica et Cartographica Sinica*, 39(5), 478–483.

[18] Zhao, X.W., Liu, C., Deng, J., Zhang, C.Y., Yu, X.X. (2016). A modified un-combined model to improve the performance of precise point positioning: model and test results. *Acta Geod Geophys*, 52(3), 1–14.

[19] Li, B.F., Ge, H.B., Shen, Y.Z. (2015). Comparison of Ionosphere-free, Uofc and Uncombined PPP Observations Models. *Acta Geodaetica et Cartographica Sinica*, 44(7), 734–740.

[20] Bona, P. (2000). Precise, Cross Correlation, and Time Correlation of GPS Phase and Code Observations. *GPS Solutions*, 4(2), 3–13.

[21] Hajiyew, C., Berberoglu, M.I. (2005). EKF based user's position estimation using GNSS measurements. *AIAC conference*. Available: *https://www.researchgate.net/publication/312161002*.

[22] Takasu, T. (2013). PPP (Precise Point Positioning). *RTKLIB ver. 2.4.2 Manual*.

[23] Cheng, Y.J., Sun, H.Y., Cheng, H.B. (2004). Robust estimate of Kalman filtering and its application in adjustment of dynamic leveling network. *Engineering of Surveying Mapping*, 13(4), 55–57.

[24] Zhou, W.W. (2000). t-test the superlative test to discard abnormal values with σ unknown. *Journal of Sichuan University of Science and Technology*, 19(3), 84–86.

[25] Brumback, B., Srinath, M. (1987). A Chi-square test for fault-detection in Kalman filters. *IEEE Transactions on Automatic Control*, 32(6), 552–554.

[26] IGS data center of Wuhan University. Available: *http://wzw.cn/index.php/Home/DataProduct/mgex.html*.